Article

The Influence of the Alkyd Composite Coatings with Polyaniline Doped by Different Organic Acids on the Corrosion of Mild Steel

Branimir N. Grgur*, Aleksandra S. Popović, Ayad A.M. Salem[ͨ]

University of Belgrade, Faculty of Technology and Metallurgy, Karnegijeva 4, 11020 Belgrade, Serbia

* Correspondence: BNGrgur@tmf.bg.ac.rs
ͨ In the memory of Ayad, 1965-2022.

Abstract: The composite coatings prepared by mixing the 5 wt.% of polyaniline with commercial alkyd-based paint are applied on carbon steel. The polyaniline emeraldine chloride salt is prepared by procedure recommended by IUPAC, deprotonated by ammonia hydroxide, and reprotonated with the sulfamic, succinic, citric, and acetic acids with different doping degrees or oxidation states. The steel samples with base and composite coatings are immersed in 3% NaCl and the corrosion current density is determined after 96 h *in-site* using ASTM 1,10-phenanthroline method. The samples are also inspected by the optical microscope. It is shown that composite coatings reduce the possibility of blister formations and delamination. The corrosion current density and the appearance of the corrosion products, which area is determined by ImageJ softer, closely follow the initial oxidation state of the polyaniline. The role of the initial state of the polyaniline is discussed. It is suggested that such behavior could be connected with the oxygen reduction reaction mechanism that proceeds mainly *via* two electron paths on the polyaniline particles, releasing a much smaller amount of hydroxyl ions, responsible for the delamination and blister formations of the commercial coatings.

Keywords: phenanthroline method; reprotonation; delamination, blistering; protection mechanism

1. Introduction

Mild steels due to their good mechanical characteristics, low price, *etc.* are common construction materials in many industries and different applications. [1, 2]. Unfortunately, it has low corrosion stability and is easily corroded in many different environments. Consequently, mild steel must be protected against corrosion, and one of the most common methods is the application of different organic coatings [3]. But over time, coatings protection characteristics decay, so many researchers investigated different additives to prolong protection, and among them conducting polymers with a main focus on polyaniline [4]

Polyaniline (PANI) due to its easy chemical or electrochemical synthesis, inexpensive monomer, distinct electrical, redox, and acid-base characteristics in addition to its various potential uses in many sectors, PANI was the subject of considerable research in the past [5, 6]. Among the other applications, a lot of effort was in the field of corrosion protection of metals and alloys. The main focus was on steel [7-9], and some other metals, like aluminum [10], magnesium alloys [11, 12] copper [13], *etc*.

Two basic polyaniline forms, the polyaniline emeraldine salt form (PANI-ES) and the polyaniline emeraldine base form (PANI-EB), are being investigated for their use as anti-corrosion coatings. Some studies have confirmed the non-conducting nature of PANI-EB and its barrier effect. On the other hand, some researchers found that PANI-EB had an anodic protective effect, while others found inconclusive results, so it is crucial to keep researching the different forms of composite PANI-based coatings on steel [7, 14-17]. The composite organic coatings containing different forms of PANI are widely investigated in the corrosion protection of metals [7, 18], but the mechanism of the corrosion protection of mild steel is still elusive [7, 19].

In our previous paper [20], the PANI composite with alkyd-based paint by different oxidation states doped with organic acids is qualitatively investigated using the linear polarization methods. It is observed that determined polarization resistance decreases with a decrease in the initial oxidation state of the polyaniline. Also, the paint blistering and delamination are suppressed to a large extent in comparison with the base coating. So, to extend that work, in this paper, we present results of the quantitatively determined corrosion rate using the ASTM International 1,10-phenanthroline standard test method and determined rust appearance on the base and composite coatings surfaces. Also, the plausible mechanism of corrosion protection is discussed in detail.
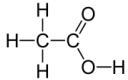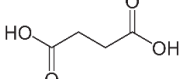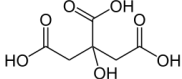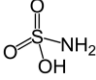
2. Materials and Methods

Polyaniline in the powdered form is produced using the chemical synthesis route suggested by the International Union of Pure and Applied Chemistry (IUPAC) guidelines [21]. In the procedure, the 0.22 mol of aniline monomer (20.5 g or 20.8 cm^3, p.a. Sigma Aldrich, previously distilled under a low-pressure condition) and 0.22 mol HCl (8 g or 26 cm^3 of 37 wt.% HCl, p.a. Merck) are well mixed at ambient temperature in 500 ml of distilled water to produce anilinium hydrochloride. Following vigorous stirring, 500 ml of 0.22 mol HCl containing 0.275 mol (62.81 g) of ammonium persulfate, $(NH_4)_2S_2O_7$, is slowly added. After 24 hours of mixing with a magnetic stirrer, the obtained green powder is filtered, repeatedly washed with 0.1 M HCl, distilled water, and acetone, and then finally dried for 24 hours in an oven at 60°C. To form the polyaniline emeraldine base (PANI-EB), a portion of the as-synthesized polyaniline emeraldine salt powder (PANI-ES) is immersed in 1 M NH$_4$OH during 24 hours under stirring conditions. The reported electrical conductivity of PANI-ES prepared by using recommended IUPAC procedure is 4.4 ± 1.7 S cm^{-1} (average of 59 samples) and for the PANI-EB electrical conductivity is 3×10^{-9} S cm^{-1} [22]. The resulting polyaniline emeraldine base powder is separately exposed in the solutions containing 0.87 M sulfamic, 1 M succinic, 1 M citric, and 1 M of acetic acid in order to produce the reprotonated polyaniline, by the route described by Stejskal et al. [22]. Typically, 100 cm^3 solutions of the appropriate acids are 24 hours continuously mixed with 2 g of the PANI-EB, and after that filtrated, rinsed with distilled water, acetone, and dried during 48 hours. Scheme 1 illustrates the reprotonotation of the polyaniline emeraldine base to emeraldine salt form with acids (HA), while Table 1 presents the characteristics of the physical-chemical data of used acids.
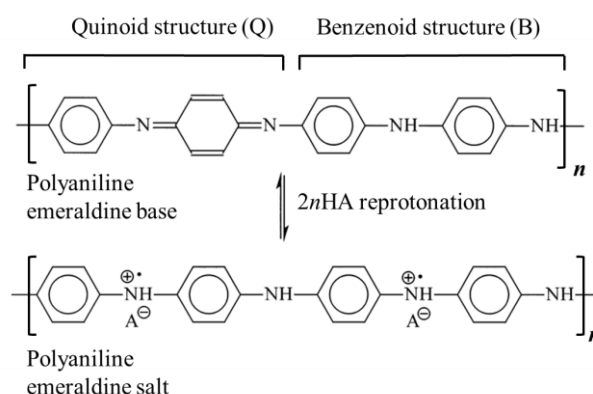
Scheme 1. The reprotonotation of the polyaniline emeraldine base to emeraldine salt form, HA organic acids.

Table 1. The characteristics data of used acids and conditions for the reprotonation of the polyaniline base form, σ-reported conductivity of reprotonated samples [22].

Acid	Structure	M_w g mol^{-1}	pK_a	c_{AC} mol dm^{-3}	pH	σ / S cm^{-1} [22]
Acetic		60.1	4.76	1	2.6	7.1×10^{-9}
Succinic		118.1	$pK_{a1} = 4.2$ $pK_{a2} = 5.6$	0.87 (sat)	2.5	5.9×10^{-6}
Citric		192.1	$pKa_1 = 3.13$ $pKa_2 = 4.76$	1	1.51	4.4×10^{-3}
Sulfamic		97.1	1.0	1	0.6	0.11

The UV-vis spectra of all PANI samples in a powdered form dispersed in distilled water (~15 mg in 20 cm^3) are obtained using LLG uniSPEC 2 spectrophotometers (Germany). The water dispersions of the polyaniline are prepared by vigorous sonication during 30 minutes, and waiting for the precipitations of larger particles for one hour.

The composite coatings containing reprotonated PANI are prepared using the commercial finishing paint for steel, "*Professional emajl lak*", Nevena Color Xemmax, Serbia, based on an alkyd binder and white pigments in organic thinners, containing 67% of solids. The mass of solids is determined by measuring the mass of wet and dry paint. The composite coating is prepared by mixing 10 g of the base paint with 5 wt.% of well grind reprotonated PANI powder, 0.33 g based on dry paint, with a particle size in the range of 0.5 to 1.0 μm. The base and composite coatings are applied using a doctor-blade method on the properly prepared samples of the low carbon, ≤ 0.13 C, mild steel (ANSI 1212) with the dimensions of 4.5 cm × 5 cm, with an exposed area of 22.5 cm^2. The backsides and the edges of the steel samples are isolated with ~200 μm thick epoxy coating. After proper drying at room temperature during 48 hours, the average coating thickness of ~25±5 μm is measured using Byko-test 4500 FE/NFe (Germany) thickness tester. The samples are separately immersed in a 200 cm^3 laboratory glass beaker containing 3% NaCl.

The corrosion rate, expressed as the average corrosion current density, of the mild steel samples painted by the base and composite coatings, as a mass of the iron in a beaker with a volume of 200 cm^3 of 3% NaCl solution, is determined after 96 hours of corrosion using the ASTM International 1,10-phenanthroline standard method [23]. The 1,10-phenanthroline reacts with ferrous ions generating an intensely colored red complex. In a typical route, after 96 hours of the corrosion, when the first corrosion product on the samples is observed, the 10 cm^3 of stack solutions are added to 100 cm^3 volumetric flasks containing 0.25 mL of concentrated sulfuric acid and ~20 cm^3 of distilled water. Then 1 cm^3 of the hydroxylamine solution, 100 g dm^3, 10 cm^3 of the 1,10-phenanthroline solution, 1 g dm^3, and 8 cm^3 of the sodium acetate solution, 1.2 M is added, respectively, and filed to 100 cm^3 with distilled water. The mass of the iron in the corrosive solutions is determined 96 hours after the immersion of the samples, by recording the UV-visible spectra using a LLG uniSPEC 2 spectrophotometer (Germany), and determining the value of the absorbance at 508 nm of investigated solutions and using the calibration line of the standard solution. Samples are left to corrode for a total of 150 hours, and the corroded area is determined from the sample images using ImageJ software [24]. For the preparation of the iron standard test solutions and determining the calibration line from UV-visible spectra, the appropriate amounts of ferrous ammonium sulfate hexahydrate, Fe(NH$_4$)$_2$(SO$_4$)$_2 \times$6H$_2$O, (Aldrich, p.a., USA) that 1.000 g contains 0.1443 g of iron, is used. The iron standard solution is prepared by dissolving 0.7022 g of ferrous ammonium sulfate hexahydrate in 500 mL of distilled water containing 20 mL of concentrated sulfuric acid and diluting to 1 L with distilled water. 100

mL of this solution is then diluted to 1 L. For the determination of the calibration curve, an adequate volume of the standard solutions is used to prepare 100 cm³ of the Fe^{2+} in the range of 18.6 µg to 0.186 mg.

The optical micrographs are acquired using an optical microscope Olympus CX41 equipped with a digital camera and connected to the PC. The image of the whole samples is obtained by PANA-SONIC DC-FZ82 digital camera

3. Results

3.1. Characterization of the samples

The UV-visible spectra of the PANI samples, sonicated in distilled water, in the range of the wavelength from ~200 to 1100 nm are presented in Figure 1. The as-synthesized PANI in the emeraldine salt form (PANI-ES), Figure 1a, has an absorption peak at 365 nm that is connected to the π–π^* transition inside the benzenoid ring (B). The peak at 440 nm can be connected to the polaron–π^* transition inside the quinoid structure (Q), followed by a broad tail associated with polaronic structures [25, 26]. The spectra of the PANI in the emeraldine base form (PANI-EB) among peak at ~365 nm, have a strong broad peak with maximum absorbance at ~700 nm that is ascribed to the molecular excitation connected with the quinoid-imine structure [26], Figure 1a. The ratio of absorbance for PANI-ES of quinoid, polaron–π^* transition at 440 nm to benzenoid, π–π^* transition at 365 nm bands can be taken as a measure of the oxidation state in the PANI conducting polymer [27-31]. All four reprotonated samples have a well-defined absorption maximum at 365 nm from π–π^* transition inside the benzenoid ring. Polyaniline doped with sulfamic acid has a shoulder at 440 nm from the polaron - π^* transition, while the other three samples have an increased absorbance, Figure 1b.
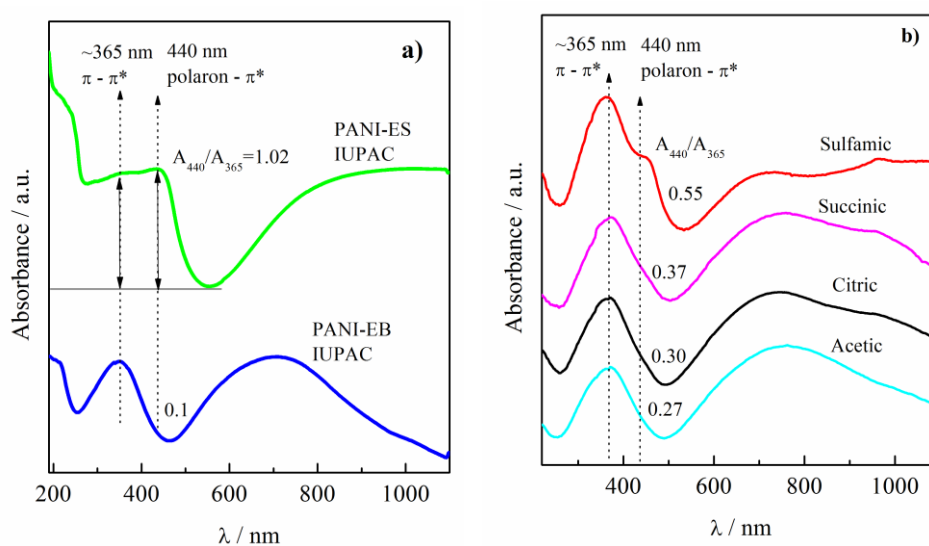

Figure 1. UV-vis spectra of a) polyaniline salt (PANI-ES) and base (PANI-EB) water dispersion synthesized according to the IUPAC recommendation, b) PANI-EB reprotonated samples with different organic acids, marked in the figure.

Figure 2 shows the polyaniline doped with sulfamic acid, particle size distribution in the composite coating, shown in the inset of Figure 2, determined using ImageJ software. It can be seen that main particle sizes are ~13±8 µm, while some agglomerates have much higher dimensions, up to 110 µm. The high agglomeration tendency of the PANI is affected by the inflexibility in the conjugated double-bond backbone and is caused by the high density of electrical charges inside the conducting polymer matrix [32]. Consequently, it is difficult to make a proper dispersion of PANI in the classical organic polymer paint which is one of the main issues in the application.
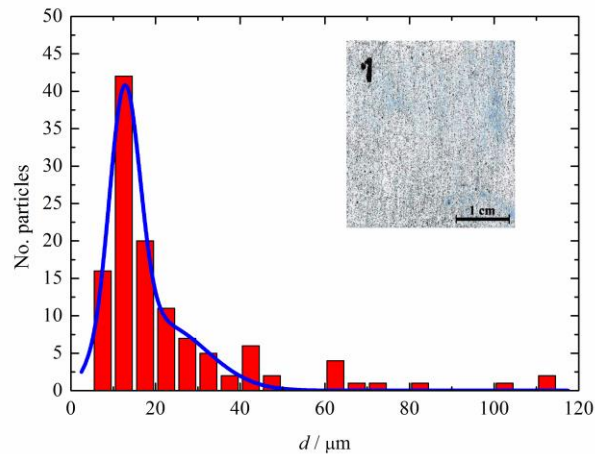
Figure 2. The particle size distribution of the polyaniline doped with sulfamic acid in the composite coating, is shown in the inset.

3.2. Corrosion behavior

The UV-visible spectra of the standard solution are shown in Figure 3a. The linear dependence of the absorption of standard solutions at 508 nm, shown in the inset of Figure 3a, is in agreement with the Lambert–Beer law. The dependence of the absorption at 508 nm over iron (iron ions) mass in grams can be given as $A = 1680\ m(Fe^{2+})$. From the Figure 3b and the inset, it can be seen that maximum absorption that corresponds to the highest iron mass in the solution, possesses base coating, then composite coatings with acetic acid; citric acid; succinic acid, and finally sulfamic acid doped polyaniline.
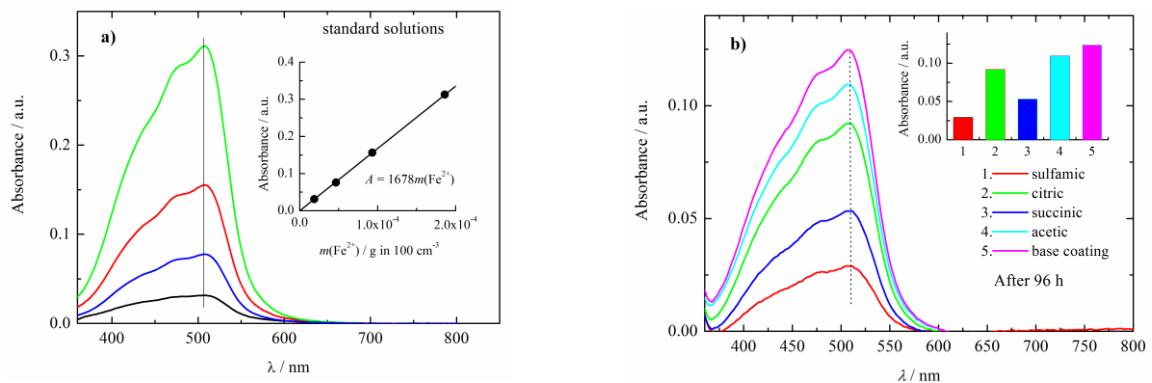

Figure 3. a) UV -vis spectra of the iron standard soltion.
Inset: calibration line b) UV-vis spectra of corrosive solution (3% NaCl) after 96 hours of immersions of the composite coatings. Inset: absorption maximum at 508 nm.

Figure 4 shows the images of the samples before, and after immersion in corrosive media, 3% NaCl, during 150 hours. The bottom images show the graphical presentation of the corroded area of the samples determined by ImageJ software. By the visual inspection, it is obvious that the steel sample with the base coating is most corroded than composite coatings with acetic acid; citric acid; succinic acid, and at last with sulfamic acid doped polyaniline, which is in agreement with UV-vis measurements.
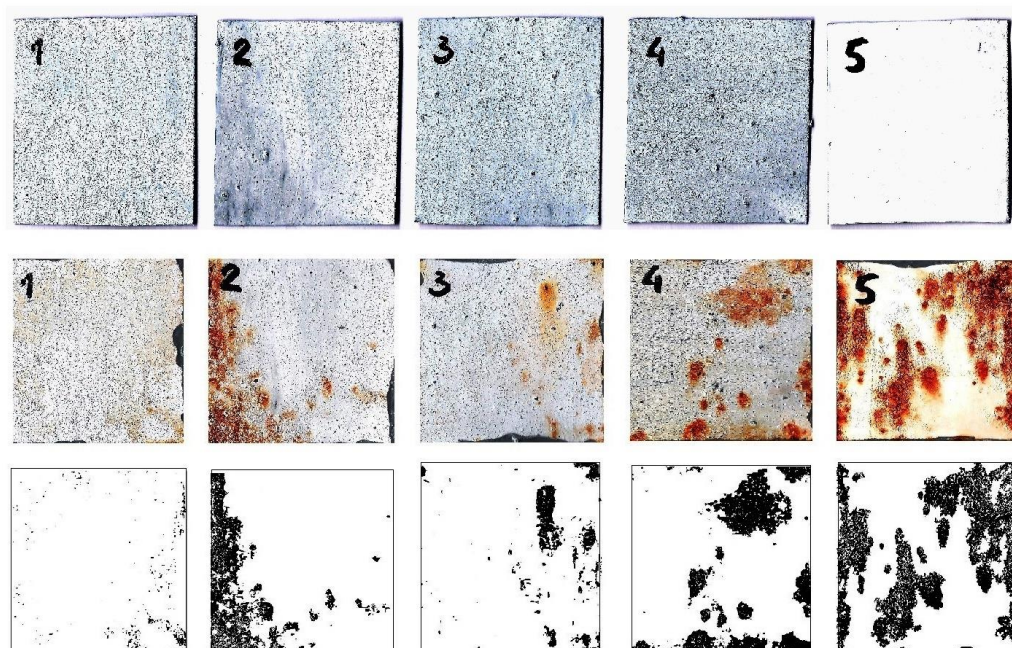
Figure 4. The images of the samples before (top), and after immersion in corrosive media, 3% NaCl, during 150 hours (middle). The bottom images show the graphical presentation of the corroded area of the samples determined by ImageJ software. Composite coatings are marked with 1-sulfamic acid; 2-citric acid; 3-succinic acid, and 4-acetic acid doped polyaniline, 5-base coating.

After exposure to corrosion media for 150 hours, the optical images of the samples with base coating and composite coating with polyaniline doped with sulfamic acid are taken and shown in Figure 5. As can be seen, the base coating is covered with huge blisters, while the composite coating shows only traces of corrosion products. Other composite coatings show the appearance of the corrosion product, but with microscope examinations, no blisters formation or delamination is observed.
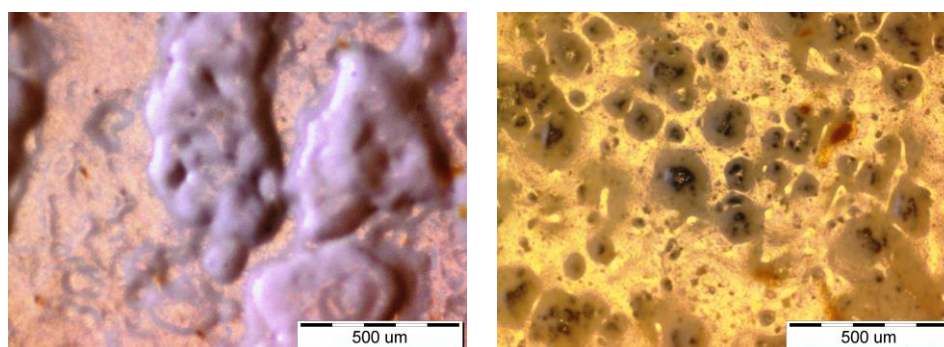

Figure 5. The optical images of the base coating (left) and composite coating with sulfamic acid doped PANI (right), after 150 hours of immersion in 3% NaCl.

4. Discussion

Protonated polyaniline theoretically can exist in three fundamental forms; fully reduced leucoemeraldine, half-oxidized emeraldine, and fully oxidized pernigraniline. From that three forms only emeraldine salt is conducive [33]. The doping degree, y, represents the average number of doped anions per polymer unit, four monomers, in the polymer chain. For example, emeraldine salt has consisted of four monomers in the polymer units and two anions, Scheme 1, so the doping degree is

0.5. Taking into account that PANI prepared following the IUPAC procedure has a doping degree of 0.5, the ratio of absorbance at 440 nm and 365 nm can be used to estimate the doping degrees of the reprotonated samples using the following equation:

$$y = \frac{(A_{440/365}) \times 0.5}{1.02} \tag{1}$$

The estimated average doping degrees of the reprotonated samples are shown in Figure 6. It can be seen that sulfamic acid doped PANI has an average doping degree of 0.27; PANI-succinic acid 0.18, PANI-citric acid 0.15, and PANI-acetic acid 0.13.
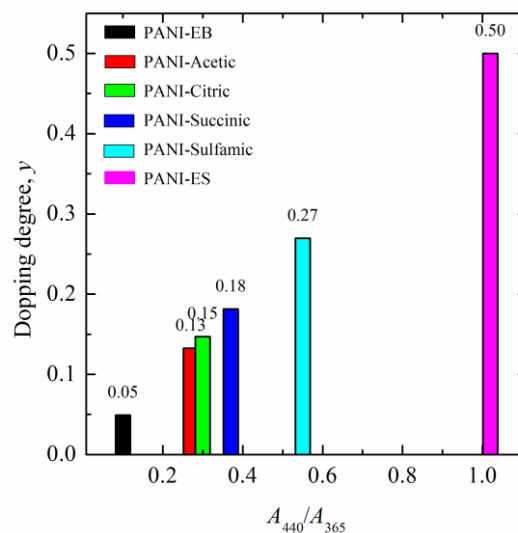

Figure 6. The estimated average doping degrees of the reprotonated samples.

To determine the corrosion rate of the base and composite coatings, from the absorbance determined after 96 hours of exposition to the corrosive solution, and taking into account calibration curve $A = 1680 \, m(Fe^{2+})$, and knowing that for the analysis is from 200 cm³ analyzed 10 cm³, the average corrosion current density is calculated using the modified equation of the Faraday law:

$$j_{corr} = \frac{A_{508} \times 20 \times n \times F}{1680 \times S \times t \times M(Fe)} \tag{2}$$

where A_{508} is absorbance after the time of immersion $t = 96$ h, inset in Figure 3b, S, cm², is the surface area of the samples, $F = 26.8$ Ah mol⁻¹ Faraday constant, and 20 is the conversion factor from 10 cm³ to 200 cm³. The calculated corrosion current density is shown in Figure 7a. It is obvious that corrosion current density closely follows the initial doping degree, and decreases with an increase of the initial doping degree. In order to compare the value of the polarization resistance with the determined j_{corr}, the same Figure 7a shows the data of the reciprocal values of the polarization resistance after 96 hours, extracted from Figure 4a from [20]. Because j_{corr} is proportional to R_P^{-1} an excellent agreement of trend is obtained using those two methods. To evaluate the formation of rust onto the surface of the sample,

Figure 7b shows the comparisons of corrosion current density with the corroded surface after prolonged immersion in 3% NaCl for 150 hours, obtained using ImageJ software, Figure 4. The close connections of the initial doping degree, j_{corr}, and appearance of the rust on the samples surfaces are obvious. For example, the base coating surface is covered with 20% of rust, while composite coatings with PANI-sulfamic acid only ~1%. Therefore, all of the investigations suggest that the initial PANI doping degree has a high influence on the corrosion protection of mild steel
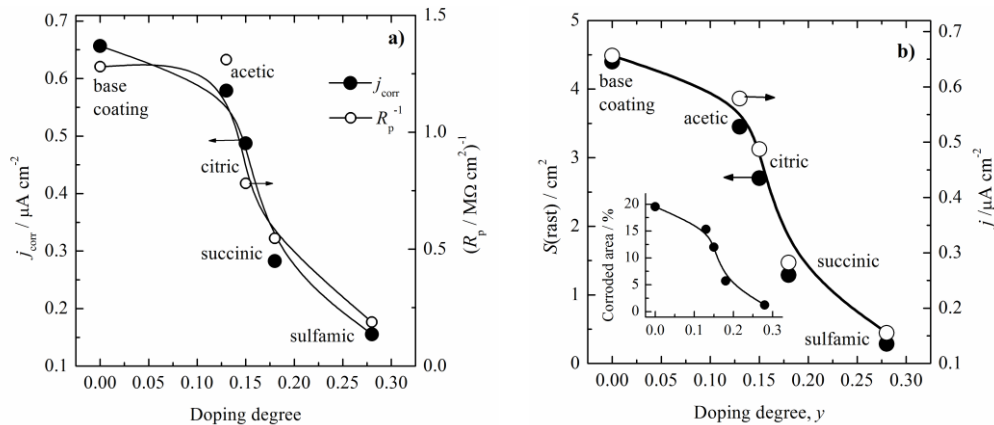

Figure 7. a) The dependence of the calculated corrosion current density and reciprocal values of polarization resistance [20] over doping degree. b) The dependence of the calculated corrosion current density and surface area of the rust formed onto the surface of the samples over the doping degree. Inset: The percentage of the corroded area of the samples over the doping degree.

The main degradation of mechanisms of the base organic coatings are delamination and the formation of blisters, as schematically shown in Figure 8 [3, 20]. During the immersion in corrosive media, the development of the pores in the coatings occurs. In the case of delamination, in the two neighboring pores, iron is dissolved, and released electrons are transferred through metal to another pore where an oxygen reduction reaction occurs producing OH^- anions, and very fast alkalization of the pore occurs, reaching pH of ~14, that provoke loss of the coating adhesion. During blister formation, oxygen, and water, penetrate through the coating, oxygen is reduced to OH^-, and with dissolved iron form rust that lifts the coatings from the steel surface.
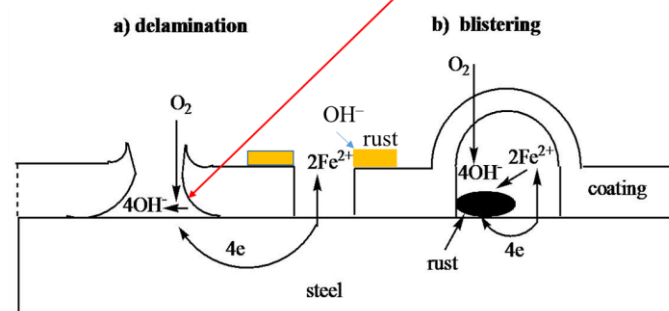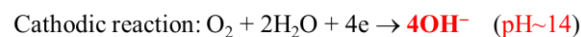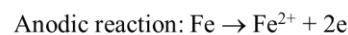

Figure 8. Schematic representations of the organic coating delamination (a) and the blister formation (b).

For polyaniline and polypyrrole is shown that could reduce oxygen to hydrogen peroxide and/or hydroxyl anions via two or four-electron path [34, 35]. Hence, it can be suggested that polyaniline with a higher doping degree and higher conductivity could reduce the oxygen to mainly hydrogen peroxide anions, HO_2^-, lowering the possibility of pH increase and formation of blisters or delamination. Decreasing the doping degree conductivity of PANI also decreases, and parallel two and four oxygen reduction paths could occur, but with a much lower concentration of OH^- and a smaller tendency of coating degradation, as schematically presented in Figure 9. It should be also mentioned that formed hydrogen peroxide anions could react with Fe^{2+} to form a passive film of Fe_2O_3 via reactions:

$$Fe^{2+} + HO_2^- + H_2O \rightarrow Fe_2O_3 + 3H^+ \tag{3}$$

and immediate reaction:

$$H^+ + OH^- \rightarrow H_2O \tag{4}$$

that again lowers the concentrations of OH^- ions in the coating pores. Also, the barrier effect on oxygen penetration due to the presence of the polyaniline particles in the composite coating should be taken into account.
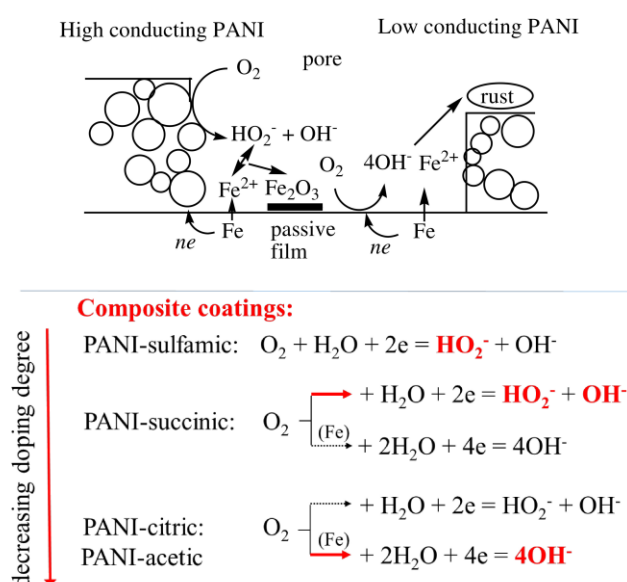

Figure 9. Simplified, nonstoichiometric, schematic representation of the possible reactions during the corrosion of the mild steel with composite polyaniline based coatings. Red arrows represent the main reactions.

5. Conclusions

In this paper, we investigated the synthesis of the polyaniline in the emeraldine salt form by the procedure suggested by IUPAC. Emeraldine salt form is deprotonated with ammonium hydroxide and reprotonated with four different organic acids. Using the UV-visible spectroscopy the doping degree is estimated. The corrosion performances of the base coating and composite coating with 5 wt.% of polyaniline doped with organic acids on mild steel are investigated by the means of *in site* determined iron concentrations in the corrosive media using ASTM 1,10-phenanthroline method and the corrosion current density is recalculated. It is also shown that the protection ability of composite coatings closely follows the initial oxidation state of polyaniline, and that polyaniline doped with sulfamic acid with doping degree of 0.27 have the best corrosion protection role. Blistering formations are suppressed in the composite coatings due to the changes in the oxygen reduction path from four to mainly two electron path. The mechanism of corrosion behavior is also discussed in detail.

References

1. Touileb, K.; Djoudjou, R.; Hedhibi, A.C.; Ouis, A.; Benselama, A.; Ibrahim, A.; Abdo, H.S.; Samad, U.A. Comparative microstructural, mechanical and corrosion study between dissimilar ATIG and conventional TIG weldments of 316L stainless steel and mild steel. *Metals* **2022**, *12*, 635. https://doi.org/10.3390/met12040635

2. Ruan, X.; Yang, L.; Wang, Y.; Dong, Y.; Xu, D.; Zhang, M. Biofilm-Induced Corrosion Inhibition of Q235 Carbon Steel by *Tenacibaculum mesophilum* D-6 and *Bacillus* sp. Y-6. *Metals* **2023**, *13*, 649. https://doi.org/10.3390/met13040649

3. Lyon, S.B.; Bingham, R.;. Mills, D.J. Advances in corrosion protection by organic coatings: What we know and what we would like to know. *Prog. Org. Coat.* **2017**, *102*, 2. https://doi.org/10.1016/j.porgcoat.2016.04.030

4. Rangel-Olivares, F.R.; Arce-Estrada, E.M.; Cabrera-Sierra, R. Synthesis and characterization of polyaniline-based polymer nanocomposites as anti-corrosion coatings. *Coatings* **2021**, *11*, 653. https://doi.org/10.3390/coatings11060653

5. Ćirić-Marjanović, G. Recent advances in polyaniline research: Polymerization mechanisms, structural aspects, properties and applications. *Synth. Met.* **2013**, *177*, 1. https://doi.org/10.1016/j.synthmet.2013.06.004

6. Ćirić-Marjanović, G. Recent advances in polyaniline composites with metals, metalloids and nonmetals. *Synth. Met.* **2013**, *170*, 31. https://doi.org/10.1016/j.synthmet.2013.02.028

7. Fangjian Gao, Jie Mu, Zhenxiao Bi, Shun Wang, Zili Li, Recent advances of polyaniline composites in anticorrosive coatings: A review, *Prog. Org. Coat.* **2021**, *151*, 106071. https://doi.org/10.1016/j.porgcoat.2020.106071

8. Hu, C.; Li, T.; Yin, H.; Hu, L.; Tang, J.; Ren, K. Preparation and corrosion protection of three different acids doped polyaniline/epoxy resin composite coatings on carbon steel. *Colloids Surf. A Physicochem. Eng. Asp.* **2021**, *612*, 126069. https://doi.org/10.1016/j.colsurfa.2020.126069

9. Zhang, Y.J.; Shao, Y.W.; Liu, X.L.; Shi, C.; Wang, Y.Q.; Meng, G.Z.; Zeng, X.G.; Yang, Y. A study on corrosion protection of different polyaniline coatings for mild steel. *Prog. Org. Coat.* **2017**, *111*, 240.

10. Liu, S.; Liu, L.; Meng, F.; Li, Y.; Wang, F. Protective performance of polyaniline-sulfosalicylic acid/epoxy coating for 5083 aluminum. *Materials* **2018**, *11*, 292. https://doi.org/10.3390/ma11020292

11. Zhang, Y.; Shao, Y.; Zhang, T.; Meng, G.; Wang, F. The effect of epoxy coating containing emeraldine base and hydrofluoric acid doped polyaniline on the corrosion protection of AZ91D magnesium alloy. *Corros. Sci.* **2011**, *53*, 3747–3755. https://doi.org/10.1016/j.corsci.2011.07.021

12. Baloch, A.; Kannan, M.B. Electropolymerisation of aniline on AZ91 magnesium alloy: The effect of coating electrolyte corrosiveness. *Metals* **2017**, *7*, 533. https://doi.org/10.3390/met7120533

13. Ma, Y.; Fan, B.; Liu, H.; Fan, G.; Hao, H.; Yang, B. Enhanced corrosion inhibition of aniline derivatives electropolymerized coatings on copper: Preparation, characterization and mechanism modeling. *Appl. Surf. Sci.* **2020,** *514*, 146086. https://doi.org/10.1016/j.apsusc.2020.146086

14. Xu, H.; Zhang, Y. A review on conducting polymers and nanopolymer composite coatings for steel corrosion protection. *Coatings* **2019**, *9*, 807. https://doi.org/10.3390/coatings9120807

15. Armelin, E.; Alemán, C.; Iribarren, J.I. Anti-corrosion performances of epoxy coatings modified with polyaniline: A comparison between the emeraldine base and salt forms. *Prog. Org. Coat.* **2009**, *65*, 88. http://dx.doi.org/10.1016%2Fj.porgcoat.2008.10.001

16. Zhang, Y.; Shao, Y.; Liu, X.; Shi, C.; Wang, Y.; Meng, G.; Zeng, X.; Yang, Y. A study on corrosion protection of different polyaniline coatings for mild steel. *Prog. Org. Coat.* **2017**, *111*, 240. https://doi.org/10.1016/j.porgcoat.2017.06.015

17. Kohl, M.; Kalendová, A. Effect of polyaniline salts on the mechanical and corrosion properties of organic protective coatings. *Prog. Org. Coat.* **2015,** *86*, 96. https://doi.org/10.1016/j.porgcoat.2015.04.006

18. Liu, T.; Wei, J.; Ma, L.; Liu, S.; Zhang, D.; Zhao, H. Effect of polyaniline-based plate on the anticorrosion performance of epoxy coating. *Prog. Org. Coat.* **2021**, *151*, 106109, https://doi.org/10.1016/j.porgcoat.2020.106109

19. Kumar, A. Role of conducting polymers in corrosion protection, *N.a. J. Adv. Res. Rev.* **2023**, **17(02**), 045. https://doi.org/10.30574/wjarr.2023.17.2.0238

20. Salem, A.J.; Grgur, B.N. The influence of the polyaniline initial oxidation states on the corrosion of steel with composite coatings. *Prog. Org. Coat.* **2018,** *119*, 138. https://doi.org/10.1016/j.porgcoat.2018.02.032

21. Stejskal, J.; Gilbert, R.G. Polyaniline: Preparation of a conducting polymer (IUPAC Technical Report). *Pure Appl. Chem.* **2002**, *74(5)* 857. https://doi.org/10.1351/pac200274050857

22. Stejskal, J.; Prokeš, J.; Trchová, M. Reprotonation of polyaniline: A route to various conducting polymer materials, *React. Funct. Polym.* **2008**, *68*, 1355. https://doi.org/10.1016/j.reactfunctpolym.2008.06.012

23. ASTM, Designation: E 394 – 00, Standard test method for iron in trace quantities using the 1,10-phenanthroline method, 2000.

24. https://imagej.nih.gov/ij/docs/guide/user-guide.pdf

25. Jin, E.; Liu, N.; Lu, X. ; Zhang, W. Novel micro/nanostructures of polyaniline in the presence of different amino acids via a self-assembly process, *Chem. Lett.,* **2007**, *36,* 1288. https://doi.org/10.1246/cl.2007.1288

26. Albuquerque de, J.E.;. Mattoso, L.H.C.; Faria, R.M.; Masters, J.G.; MacDiarmid, A.G. Study of the interconversion of polyaniline oxidation states by optical absorption spectroscopy. *Synth. Met.* **2004**, *146*, 1. https://doi.org/10.1016/j.synthmet.2004.05.019

27. Sk, M.M.; Yue, C.Y. Synthesis of polyaniline nanotubes using the self-assembly behavior of vitamin C: a mechanistic study and application in electrochemical supercapacitors, *J. Mater. Chem. A* **2014**, *2*, 2830. https://doi.org/10.1039/C3TA14309K

28. Han, Y-G.; Kusunose, T.; Sekino T. One-step reverse micelle polymerization of organic dispersible polyaniline nanoparticles, *Synth. Met.* **2009**, *159,* 123. https://doi.org/10.1016/j.synthmet.2008.08.011

29. Wang, X.; Li, Y.; Zhao, Y.; Liu, J.; Tang, S.; Feng W. Synthesis of PANI nanostructures with various morphologies from fibers to micromats to disks doped with salicylic acid. *Synth. Met.* **2010**, 160, 2008. https://doi.org/10.1016/j.synthmet.2010.07.030

30. Prevost, V.; Petit, A.; Pla, F. Studies on chemical oxidative copolymerization of aniline and o-alkoxysulfonated anilines: I. Synthesis and characterization of novel self-doped polyanilines. *Synth. Met.* **1999**, *104*, 79. https://doi.org/10.1016/S0379-6779(99)00009-0

31. Xia, H.; Wang Q. Synthesis and characterization of conductive polyaniline nanoparticles through ultrasonic assisted inverse microemulsion polymerization, *J. Nanopart. Res*. **2001**, *3,* 401. <u>http://dx.doi.org/10.1023/A:1012564814745</u>

32. Bertuoli, P.T.; Baldissera, A.F.; Zattera, A.J.; Ferreira, C.A.; Alemán, C.; Armelin, E. Polyaniline coated core-shell polyacrylates: Control of film formation and coating application for corrosion protection. *Prog. Org. Coat.* **2019**, *128,* 40. <u>https://doi.org/10.1016/j.porgcoat.2018.12.007</u>

33. Beygisangchin, M.; Abdul Rashid, S.; Shafie, S.; Sadrolhosseini, A.R.; Lim, H.N. Preparations, properties, and applications of polyaniline and polyaniline thin films—A Review. *Polymers* **2021**, *13*, 2003. <u>https://doi.org/10.3390/polym13122003</u>

34. Rabl, H.; Wielend, D.; Tekoglu, S.; Seelajaroen, H.; Neugebauer, H.; Heitzmann, N.; Apaydin, DH.;, Scharber, MC.; Sariciftci, NS. Are polyaniline and polypyrrole electrocatalysts for oxygen (O_2) reduction to hydrogen peroxide (H_2O_2)? *ACS Appl Energy Mater*. **2020**, *3(11),*:10611. <u>https://doi.org/10.1021/acsaem.0c01663</u>

35. Grgur, B.N. Metal | polypyrrole battery with the air regenerated positive electrode. *J. Power Sources*, **2014,** *272*, 1053. <u>https://doi.org/10.1016/j.jpowsour.2014.09.033</u>